



OPEN

Effect of jaw width in jaw tracking mode on the radiotherapy dose of partial arc VMAT in patients undergoing left breast-conserving surgery

Hai-liang Guo^{1,5}, Yan Huan^{2,5}, Jing-hua Zhong¹✉, Hao-wen Pang³✉ & Huai-wen Zhang⁴✉

To analyze the effect of jaw width in jaw tracking mode on the dose of radiotherapy partial arc VMAT (P-VMAT) for patients undergoing left breast-conserving surgery and to explore the best jaw width as the initial inverse optimization parameter. Twenty patients who underwent left breast-conserving surgery were randomly selected. Six groups of P-VMAT plans were designed (named Plan0, Plan0.3, Plan0.6, Plan0.9, Plan-0.3, and Plan-0.6). The width of the jaw of each plan was changed in 0.3 cm steps along the X direction (from -0.6 to 0.9 cm) according to the beginning of the half beam (Plan0). The PTV coverage, conformity index (CI), homogeneity index (HI), monitor units (MU) and organs at risk (OARs) dose were evaluated by repeated measurement data analysis of variance between plan0 and the other plans. Additionally, the correlations between CI, HI, MU and OARs to change in jaw width were analyzed using Spearman's bivariate correlation analysis. The PTV dose distributions of Plan-0.3 and Plan-0.6, which have smaller jaw widths than those of Plan0, did not meet the clinical requirements. CI, HI and MU were correlated with jaw width ($r=0.554, -0.501, -0.641, p<0.05$, respectively). The V5, V10, V20, V40, Dmean and Dmax of the heart were correlated with jaw width ($r=0.288, 0.284, 0.191, -0.27, 0.186, -0.245, p<0.05$, respectively). The V2.5, V5, V10, V20, V40 and Dmean of the left lung (Lung-L) were correlated with jaw width (0.298, 0.421, 0.516, 0.391, -0.241, 0.356, $p<0.05$, respectively). Among all the plans to ensure PTV target coverage, Plan0 had the lowest clinical indicators for the heart and Lung-L ($p<0.05$, respectively). The internal boundary of the jaw set as 0 cm (Plan0) represents the optimal jaw width for the initial optimization of the plan design. This method is the simplest and most effective for radiotherapy treatment planning for breast-conserving surgery for breast cancer as well as allows ideal dose distribution.

Keywords Left breast-conserving surgery, Partial arc VMAT, Jaw width, Organ at risk, Dosimetry

Breast cancer is the most common malignancy in women¹. Breast-conserving surgery (BCS) for early-stage breast cancer has become the standard treatment. After surgery, sequential tumor bed boost radiotherapy for the whole breast can reduce the risks of local recurrence and mortality². The common complications of breast radiotherapy are radiation-related heart injury and lung injury, which are prone to cause secondary tumors³. Three-dimensional conformal radiation therapy (3D-CRT), intensity-modulated radiotherapy (IMRT), and volumetric modulated arc therapy (VMAT) have been used to treat breast cancer. The 3D conformal field in the field technique can make the radiotherapy dose to the breast more uniform⁴, but this technology may not be able to achieve full target coverage, and it brings a greater risk of giving a dose to organs at risk (OARs)⁵.

¹Department of Oncology, Jiangxi Clinical Research Center for Cancer, the First Affiliated Hospital of Gannan Medical University, First Clinical Medical College, Gannan Medical University, Ganzhou 341000, China. ²Department of Oncology, People's Hospital of Qianxinan Buyi and Miao Minority Autonomous Prefecture, Qian xinan, Xingyi 562400, China. ³Department of Oncology, The Affiliated Hospital of Southwest Medical University, Luzhou 646000, China. ⁴Department of Radiotherapy, Jiangxi Clinical Research Center for Cancer, Jiangxi Cancer Hospital & Institute, The Second Affiliated Hospital of Nanchang Medical College, Nanchang 330029, China. ⁵Hai-liang Guo and Yan Huan contributed equally to this work. ✉email: 413623991@qq.com; haowenpang@foxmail.com; 1761580890@qq.com

IMRT technology can improve the dose distribution in the target area and reduce the dose to OARs using an inhomogeneous intensity modulated beam^{6,7}.

The use of multileaf collimation (MLC) to adjust the in-field intensity prolongs the treatment time, and breathing movement and displacement within the treatment fraction increase dose uncertainty^{8,9}. Compared with IMRT, VMAT for breast cancer can improve the coverage of the planning target volume (PTV), reduce the dose received by the lung and heart on the diseased side, reduce the total number of MU, shorten the treatment time, and reduce the effects of changes in breast volume on overall tumor coverage^{10,11}. Full arc or half arc VMAT can not only increase the low-dose volume of the contralateral lung, breast and heart but also increase the risk of second cancer^{12–14}. Virén, Pasler, et al. compared the 50–60° partial arc VMAT technique (P-VMAT)¹⁵ with full-arc or half-arc VMAT, and the results showed that the partial-arc technique improved dose projection accuracy by increasing the mean open field area at the beam control point while reducing the dose and volume of radiation to OARs on the contralateral side. Fogliata et al. studied the risk assessment of secondary cancers between VMAT and 3D-CRT radiotherapy techniques for breast cancer and reported that P-VMAT was as good as 3D-CRT at avoiding sectors, and it reduced the acute and late NTCP levels in the affected organs¹⁶.

The Eclipse 3D treatment planning system (version 15.5, Varian, USA) uses jaw tracking technology in VMAT to achieve jaw movement after MLC movement, which can significantly reduce leakage between the MLC leaves and the dose received by the surrounding OARs^{17,18}. The maximum width of the open jaw at each beam control point is determined by the set starting position. Different jaw widths have a significant impact on the dosimetry and complexity of VMAT plans. An increased jaw width improves projection efficiency but reduces the protection of the OARs^{19–21}. To date, VMAT plans for breast cancer focus on the number of rotation arcs, starting angle, and beam avoidance area in most cases^{22,23}; additionally, either the starting position of the jaw is usually set as the automatically conformal target volume or the size of the jaw in the X direction should be set to not exceed 15 cm to ensure good modulation ability and projection efficiency of the beam^{24,25}. No study of the dosimetric effects of different jaw widths on breast cancer target areas and surrounding OARs has been reported. This study analyzed the dosimetry influence of different jaw widths on the results of P-VMAT after left breast conserving surgery under jaw tracking mode and proposed the initial optimization optimal jaw width to provide a reference for clinical treatment.

Materials and methods

General patient information

Twenty female patients who underwent left breast-conserving surgery and who were admitted to the radiation therapy department of our hospital between January 2022 and December 2023 were randomly selected. Pathology revealed 16 cases of invasive carcinoma, one case of high-grade ductal carcinoma in situ, one case of intermediate-grade ductal carcinoma, one case of carcinoma in situ, and one case of mucinous carcinoma. In terms of TNM stage, 15 patients had T1N0M0 disease, four patients had T2N0M0 disease, and one patient had T3N0M0 disease. No patient had any other high-risk factors. After surgery, the left whole breast and tumor bed needed only boost radiotherapy. The median age was 45 years (36–60 years), and the median breast glandular target volume was 611.1 cm³ (314.6–996.8 cm³). No patient had any contraindications to radiotherapy. According to the ethical guide-lines of the Helsinki Declaration and was approved by the institutional review board of the First Affiliated Hospital of Gannan Medical University. Written informed consents were obtained from all patients prior to treatment.

CT scan and target volume delineation

All patients were fixed in a breast bracket and a vacuum negative-pressure cushion (Model R610-DCF 1, Klarify Company, China), with the head in the center and the hands raised and outstretched. Markers were established to affix lead pellets in the stable areas of the chest skin that are less affected by respiratory movements and arm movement. A free-breathing CT scan was performed on a 16-detector CT simulator (Model Discovery RT, GE, USA) with a scan voltage of 120 kV, current of 240 mAs, and layer thickness of 2.5 mm. The CT images were reconstructed and transmitted to an Eclipse 15.5 3D treatment planning system. The clinical target volume (CTV) was the whole breast tissue volume measured on CT with the assistance of wire markers, which were placed around the palpable breast tissue during the simulation. The CTV was limited posteriorly to the intercostal front and 5 mm from the skin. The boost region (GTVtb) encompassed the surgical bed or seroma. The PTV and PTVtb were expanded 5 mm based on the CTV and GTVtb, excluding the heart. According to the RTOG 1005, NCT04025164 protocol and Guideline of target delineation and treatment planning of adjuvant radiotherapy for breast cancer of China National Cancer Center^{26–28}, in order to remove most of the buildup region for optimizing and evaluating dose, PTV and PTVtb should be expanded by 0.5 cm in all directions on the basis of CTV and GTVtb, respectively, and limited to a range of 0.5 cm below the skin surface and restricted posteriorly to the intercostal anterior region. The contoured OARs were the left lung (Lung-L), heart, right breast (Breast-R), right lung (Lung-R), spinal cord, and trachea. According to the dose-partitioning method reported by Wang et al., P-VMAT was used to irradiate the breast PTV at a prescribed dose of 42.56 Gy, and 16 fractions were completed²⁹.

Study design

To compare the dosimetric effect of the change in jaw width in jaw tracking mode for patients after breast-conserving surgery, we developed six groups of P-VMAT plans by changing the starting jaw width in steps of 0.3 cm (named Plan0, Plan0.3, Plan0.6, Plan0.9, Plan-0.3, and Plan-0.6). With reference to the report by Boman et al.²², the isocenter of the radiation field was placed on the median transverse section CT image of their planning target volume (PTV). The midpoint of the line between the medial boundary and the lateral boundary of the PTV target area was the isocenter of the radiation field to reduce the effect of the beam divergence angle on

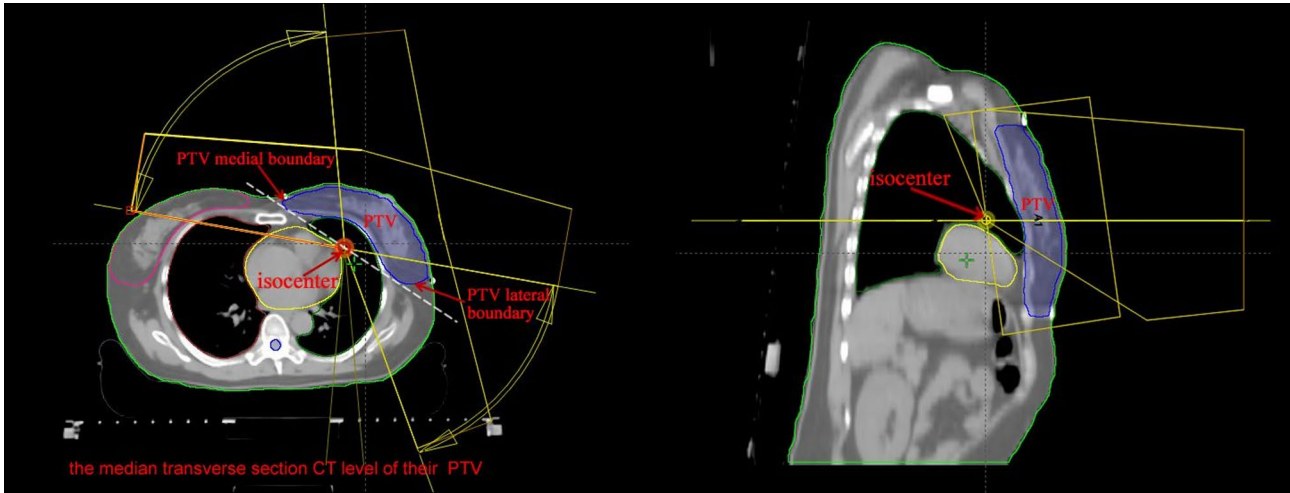


Fig. 1. P-VMAT isocenter setup.

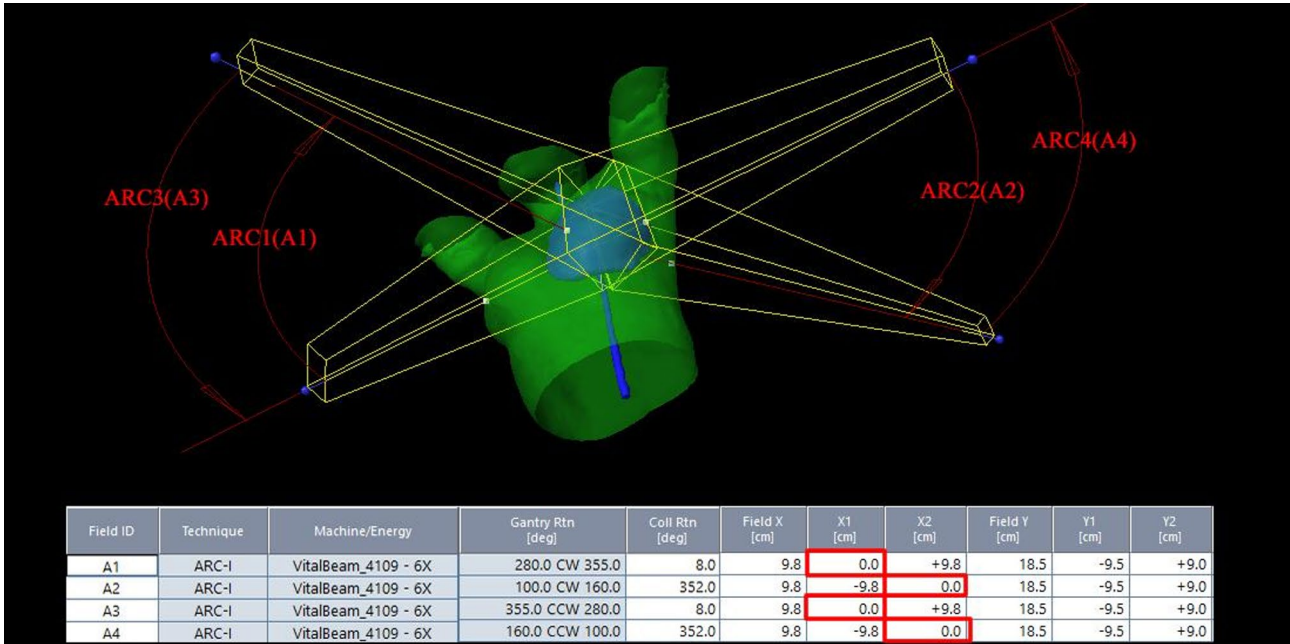


Fig. 2. Arc of rotation, collimator and Plan0 jaw setting (jaw X2 was set to 0 cm from 160° to 100° in counterclockwise and inverse partial arcs, and jaw X1 was set to 0 cm from 280° to 355° in clockwise and inverse partial arcs).

the healthy lung and breast (Fig. 1). Four partial arcs were used to design six groups of P-VMAT plans. According to the shape of the breast PTV, the first partial arcs were rotated 160°~165° to 100°~95° counterclockwise and its inverse. Second partial arcs were rotated 280°~285° to 350°~355° clockwise and its inverse, with a collimator at an angle of 0°~10° to ensure that the bottom edge of the jaw was parallel to the thoracic alignment to reduce radiation to the ipsilateral lung. In Plan0, the starting position of the jaw was set to the automatic conformal PTV to ensure that the PTV was exposed throughout the partial arc. Then, the internal boundary of the jaw (jaw X2) was set to 0 cm from 160°~165° to 100°~95° in counterclockwise and inverse partial arcs. In contrast, the internal boundary of the jaw (jaw X1) was set to 0 cm from 280°~285° to 350°~355° in clockwise and inverse partial arcs (Fig. 2). Compared with those in plan0, the jaws in the X2 direction are 0.3 cm, 0.6 cm, 0.9 cm, -0.3 cm and -0.6 cm (from 160°~165° to 100°~95° of the partial arc), while the jaws in the X1 direction are -0.3 cm, -0.6 cm, -0.9 cm, 0.3 cm and 0.6 cm (from 280°~285° to 350°~355° of the partial arc) in plan0.3, plan0.6, plan0.9, plan-0.3 and plan-0.6, respectively; other settings are consistent with plan0. Plan0 was taken as the reference, and the jaw widths in the X direction of Plan0.3, Plan0.6, Plan0.9, Plan-0.3, and Plan-0.6 were increased by 0.3 cm, 0.6 cm, 0.9 cm, -0.3 cm, and -0.6 cm, respectively (Fig. 3). The jaw width in all plans in the x direction did not exceed

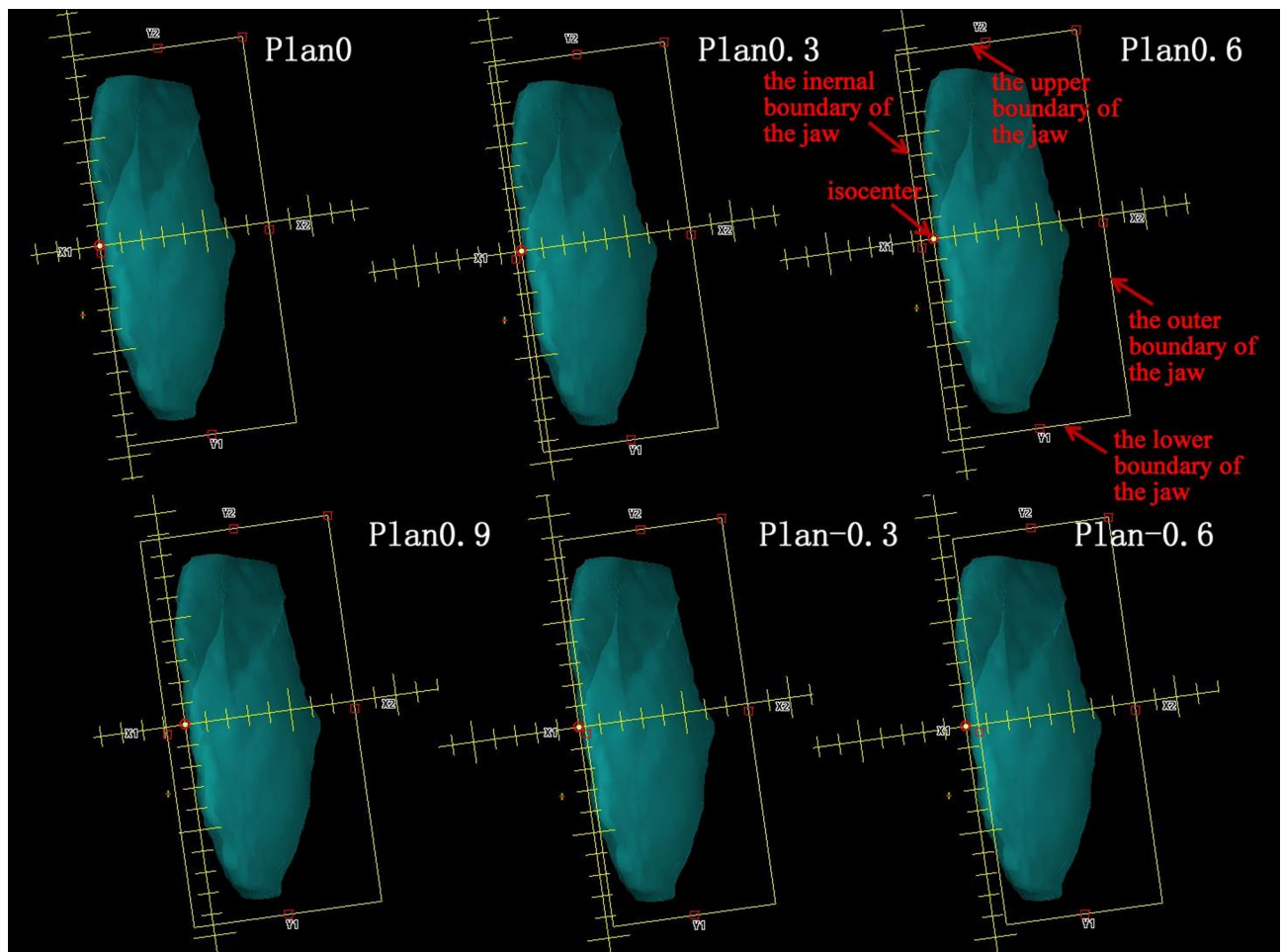


Fig. 3. Six plans Jaw setup and relative position of the jaw and PTV when the gantry is rotated to the tangential direction for the six plans in 280°~285° to 350°~355° arc segments.

15 cm. For the same patient, all six plans maintained the same initial objective function and weight in reverse optimization. Since it was required that at least 95% of the PTV volume should accept 100% of the prescribed dose, the weight of PTV can be adjusted appropriately to achieve the clinical dose target, but the objective function and weight parameters of OARs remain unchanged throughout the optimization process. With reference to the method proposed by Rossi et al., a 10-mm virtual bolus was used in the optimization design to open the MLC leaf in the air outside the target volume to compensate for the decreased dose coverage of the target region caused by respiratory movement, breast edema or breast deformation³⁰, and this virtual bolus was removed from the final dose calculation. A Varian VitalBeam linear accelerator with a 6-MV photon energy beam, Millennium 120 leaf MLC, jaw tracking mode, and 600 MU/min dose rate was used. Photon optimization types were used to optimize the VMAT plans, and dose calculations were performed with the Acuros XB algorithm with a 2.5-mm computational grid. By dose normalization, 95% of the PTV in all plans received 100% of the prescribed dose. The dose volume of the prescribed dose when exposed to more than 107% is less than 10%, the dose volume of the prescribed dose when exposed to more than 110% is less than 1%, the maximum dose to OARs (the Spinal cord and Trachea) was less than 30 Gy, the average dose to the contralateral breast was less than 4 Gy, the average dose to the lung on the ipsilateral side was less than 10 Gy, V20 < 20%, V5 < 40%, the contralateral lungs received V5 < 20%, and the average dose to the heart was less than 5 Gy, V20 < 5%, and V10 < 30%.

Acquisition of dose parameters

The PTVs and doses to the OARs of the six P-VMAT plans were assessed using a 3D dose-volume histogram (DVH) and relevant dosimetric data provided by Varian Eclipse 15.5 3D TPS.

Program evaluation

The dose received by the most exposed 2% of the PTV was regarded as the maximum dose (D2%), and the dose received by 98% of the PTV was regarded as the minimum dose (D98%). The mean dose (Dmean), median dose (D50%), monitor units (MU), and PTV volume percentages (V95, V107, and V110) for 95%, 107%, and 110% of the prescription dose, respectively, were recorded. The conformity index (CI) and homogeneity index (HI)

of the PTV target volume were based on the recommendations of the International Commission on Radiation Units and Measurements (ICRU) 83 report³¹:

$$CI = \frac{V_{T,ref}}{V_T} \times \frac{V_{T,ref}}{V_{ref}} \quad (1)$$

where $V_{T,ref}$ is the volume of the PTV that receives the prescribed dose, V_T is the volume of the PTV, V_{ref} is the total volume that receives the prescribed dose, and CI ranges from 0~1. The closer the CI is to 1, the more conformal the target volume is.

$$HI = (D2\% - D98\%) / D50\% \quad (2)$$

The closer the HI is to 0, the more uniform the target volume. The V2.5, V5, V10, V20, V30, V40, and Dmean of the left lung (Lung-L) and the heart. The Dmax of the heart; the V5, V2.5, and Dmean of the right lung (Lung-R); the V5, V10, Dmean, and Dmax of the right breast (Breast-R); and the Dmean and Dmax of the spinal cord and trachea were recorded, where V_x represents the volume exposed to dose X, and Dmean and Dmax represent the mean dose and the maximum dose to OARs, respectively.

Correlation analysis

The correlation of the PTV and OAR indicators and the jaw width were used to reverse-map the effect and variation trend of the jaw width on the doses received by the PTV and OARs.

Statistical methods

All DVH data were input into and analyzed by SPSS 16.0. Quantitative data are expressed as the mean \pm standard deviation ($\bar{x} \pm s$). The correlations between two variables were analyzed via Spearman's bivariate correlation, and two related samples were compared via repeated measurement data analysis of variance with a p value < 0.05 indicating a statistically significant difference.

Results

PTV dosimetry

The statistical indicators of the PTV are shown in Table 1. The D98% and V95 of Plan-0.3 and Plan-0.6 decreased to a greater extent than did those of Plan0, suggesting that the dose coverage of the target volumes decreased. The CI of Plan-0.3 and Plan-0.6 decreased, D2%, V107, V110, D50%, HI, and MU increased, the high-dose volume of the tumor target area increased, the uniformity decreased, and the dose delivery efficiency also decreased (all $P < 0.05$). The average DVH curves of the PTVs for the six groups of plans in Fig. 4 also showed that Plan-0.3 and Plan-0.6 could not meet the clinical requirements of a V107 less than 10% and a V110 less than 1%.

Dose to oars

Table 1 also lists the statistical indicators of the OARs and a comparison between Plan0 and the other groups. The average DVH curves for each OAR are shown in Fig. 5. The differences between the Plan0 group and the other groups for the heart, left lung, right breast and spinal cord were significant ($P < 0.05$), while the differences for the right lung and trachea were not significant ($P > 0.05$).

Correlation analysis

The mean CI, HI, and MU versus jaw width are shown in Fig. 6. CI, HI, and MU were correlated with increasing jaw width ($r = 0.554$, -0.501 , and -0.641 , respectively, $P < 0.05$). Figure 7 shows that the heart and Lung-L mean values change with jaw width. The V5, V10, V20, and Dmean of the heart were positively correlated with increasing jaw width ($r = 0.288$, 0.284 , 0.191 , and 0.186 , respectively; $P < 0.05$). The V40 and Dmax of the heart were negatively correlated with the increase in jaw width ($r = -0.27$ and -0.245 , respectively, $P < 0.05$). Lung-L V2.5, V5, V10, V20, and Dmean were positively correlated with the increase in jaw width ($r = 0.298$, 0.421 , 0.516 , 0.391 , and 0.356 , respectively; $P < 0.05$). The V40 of the Lung-L was negatively correlated with the increase in jaw width ($r = -0.241$, $P < 0.05$).

Discussion

In this study, we used a stepped jaw width of 0.3 cm as a variable to design six-group plans to determine the optimal width interval of P-VMAT for patients after BCS. When the field width relative to Plan0 is less than 0.6 cm, the plan coverage of the PTV in most patients does not meet clinical requirements. Moreover, two important organs at risk, the left lung and the heart, were positively correlated with jaw width. Therefore, in the planning group, the change interval of the jaw width was only designed to be 0.9 cm to -0.6 cm. Compared with those of Plan0, the dose coverage of the target areas of Plan-0.3 and Plan-0.6 significantly decreased, the CI of the target areas worsened, and the uniformity and dose projection efficiency also decreased. This may be because the average open area of the jaw is mainly in the tangential direction^{32,33}. When the gantry is rotated in the tangential direction, due to the small jaw width, some parts of the target volumes are outside the jaw, and the plan cannot meet the clinical requirements. If the direction other than the tangent was taken as the main direction of PTV exposure, the dose to the left lung and heart would greatly increase. When the jaw width is greater and the internal boundary of the jaw in the tangential direction exceeds the medial boundary of the PTV, the distance between the movement of the internal boundary of the jaw and the medial boundary of the PTV is greater, the MLC leakage more, which leads to low-dose-volume linearity in the heart and left lung. This may

Structure	Parameters	Plan0.9	Plan0.6	Plan0.3	Plan0	Plan-0.3	Plan-0.6
PTV	V95 (%)	99.26 ± 0.23	99.26 ± 0.23	99.2 ± 0.25	99.22 ± 0.28	98.9 ± 0.45*	98.31 ± 1.01*
	V107 (%)	4.81 ± 2.76	4.26 ± 2.55	4.12 ± 2.63	4.28 ± 2.47	10.36 ± 8.06*	39.0 ± 32.07*
	V110 (%)	0.09 ± 0.15	0.09 ± 0.12	0.12 ± 0.19	0.13 ± 0.16	1.65 ± 2.39*	19.71 ± 27.87*
	D98% (cGy)	4161.3 ± 12.97	4161.8 ± 13.84	4159.9 ± 15.84	4159.4 ± 15.64	4134.6 ± 38.42*	4016.3 ± 269.92*
	D2% (cGy)	4582.6 ± 29.59	4578.5 ± 29.15	4578 ± 26.52	4581.8 ± 25.11	4644.2 ± 76.52*	4831.4 ± 276.3*
	Dmean (cGy)	4408.2 ± 15.24	4405 ± 13.36	4403.7 ± 15.56	4402.2 ± 16.62	4425.9 ± 30.29*	4538 ± 162.19*
	D50% (cGy)	4409.9 ± 15.8	4407.2 ± 13.96	4406.2 ± 17.29	4403.7 ± 19.55	4427.8 ± 32.11*	4553.3 ± 181.18*
	CI	0.88 ± 0.02*	0.88 ± 0.02*	0.87 ± 0.02*	0.86 ± 0.02	0.85 ± 0.03*	0.81 ± 0.05*
	HI	0.09 ± 0.01	0.09 ± 0.01	0.09 ± 0.01	0.1 ± 0.01	0.12 ± 0.02*	0.18 ± 0.1*
	MU	874 ± 96.11*	911.5 ± 116.66*	959.9 ± 134.17*	1026.8 ± 168.13	1148 ± 174.82*	1235.7 ± 207.05*
Heart	V40 (%)	0.04 ± 0.08	0.07 ± 0.14	0.11 ± 0.21	0.11 ± 0.19	0.24 ± 0.33*	0.33 ± 0.44*
	V30 (%)	1.0 ± 0.94	1.0 ± 0.93	1.07 ± 0.99	1.03 ± 0.92	1.03 ± 1.05	0.91 ± 0.93
	V20 (%)	2.68 ± 2.17*	2.58 ± 2.0*	2.54 ± 1.96*	2.32 ± 1.77	2.0 ± 1.76*	1.59 ± 1.43*
	V10 (%)	5.1 ± 3.52*	4.85 ± 3.17*	4.68 ± 3.16*	4.09 ± 2.75	3.4 ± 2.58*	2.73 ± 2.16*
	V5 (%)	8.06 ± 5.01*	7.74 ± 4.48*	7.36 ± 4.46*	6.37 ± 3.83	5.56 ± 3.65*	4.84 ± 3.31*
	V2.5 (%)	16 ± 8.17*	15.64 ± 7.68*	15.37 ± 7.63*	14.53 ± 7.19	13.89 ± 7.48*	13.42 ± 7.1*
	Dmean (cGy)	236.69 ± 108.33*	232.17 ± 100.42*	230.28 ± 100.93*	218.08 ± 91.32	205.94 ± 93.42*	193.62 ± 84.45*
	Dmax (cGy)	3797.2 ± 668.67*	3867.2 ± 662.91	3903 ± 709.37	3912.8 ± 691.56	4011.5 ± 770.8*	4170.9 ± 971.83*
Lung-L	V2.5 (%)	38.17 ± 4.72*	37.53 ± 4.67*	36.68 ± 4.65*	35.57 ± 4.69	34.48 ± 4.85*	34.23 ± 4.78*
	V5 (%)	24.5 ± 3.81*	24.0 ± 3.80*	23.32 ± 3.77*	22.31 ± 3.85	21.27 ± 3.97*	20.59 ± 3.9*
	V10 (%)	17.08 ± 3.4*	16.78 ± 3.33*	16.25 ± 3.29*	15.28 ± 3.41	14.07 ± 3.61*	13.03 ± 3.52*
	V20 (%)	11.59 ± 2.87*	11.45 ± 2.8*	11.26 ± 2.79*	10.73 ± 2.81	9.9 ± 3.0*	8.95 ± 3.06*
	V30 (%)	7.17 ± 2.45	7.18 ± 2.45	7.27 ± 2.44	7.12 ± 2.51	6.92 ± 2.72	6.46 ± 2.68*
	V40 (%)	1.63 ± 1.42*	1.67 ± 1.33	1.87 ± 1.5	1.96 ± 1.74	2.49 ± 2.23*	3.05 ± 2.35*
	Dmean (cGy)	625 ± 110.38*	618.03 ± 109.01*	609.65 ± 108.38*	589.01 ± 111.60	566.87 ± 121.5*	547.46 ± 122.39*
Lung-R	V5 (%)	0.01 ± 0.22	0.01 ± 0.45	0.01 ± 0.45	0.0 ± 0.0	0.0 ± 0.0	0.0 ± 0.0
	V2.5 (%)	0.07 ± 0.16	0.07 ± 0.18	0.09 ± 0.22	0.07 ± 0.16	0.07 ± 0.14	0.06 ± 0.17
	Dmean (cGy)	15.40 ± 6.89	15.50 ± 6.98	16.38 ± 8.06	16.26 ± 7.64	16.65 ± 8.22	16.16 ± 7.65
Breast-R	V5 (%)	2.54 ± 3.45	2.66 ± 3.43	2.95 ± 3.95	2.92 ± 4.06	3.51 ± 4.57*	3.67 ± 4.28*
	V10 (%)	0.39 ± 0.99*	0.45 ± 1.06*	0.64 ± 1.61*	0.81 ± 1.92	1.01 ± 2.08*	1.01 ± 1.90
	Dmean (cGy)	63.64 ± 41.19	65.05 ± 41.66	68.69 ± 49.01	69.6 ± 54.72	77.51 ± 60.16*	77.25 ± 55.8
	Dmax (cGy)	1002.7 ± 604.47*	1033.6 ± 611.45*	1089.3 ± 623.53	1117.8 ± 673.18	1153.4 ± 720.08	1208.9 ± 664.73*
Spinal cord	Dmax (cGy)	35.11 ± 8.94	34.47 ± 8.5	34.47 ± 8.16	34.26 ± 8.78	33.41 ± 8.08	34.26 ± 8.45
	Dmean (cGy)	13.70 ± 5.05*	13.41 ± 4.92*	12.95 ± 4.5*	12.53 ± 4.36	12.14 ± 4.34*	11.72 ± 4.53*
Trachea	Dmax (cGy)	64.05 ± 18.55	63.63 ± 18.55	63.63 ± 17.6	64.27 ± 17.41	63.63 ± 18.29	65.97 ± 17.82*
	Dmean (cGy)	36.08 ± 12.88	36.29 ± 13.03	36.25 ± 12.25	36.47 ± 11.95	36.31 ± 12.19	36.7 ± 11.72

Table 1. Dose comparison of the PTVs of the six groups. *Statistically significant difference ($p < 0.05$) in pairwise comparisons against Plan0.

also explain why the V5, V10, V20, and Dmean of the heart and the left lung were positively correlated with increasing jaw width.

Darby et al. reported that the incidence of radiation myocarditis caused by radiotherapy for breast cancer increases linearly with the average dose to the heart, with a significant increase of 7.4% for every 1 Gy increase, and there is no significant threshold³. Therefore, it is particularly important to minimize the received dose and volume of the heart while ensuring that the dose reaches the target region. This study revealed that the average dose to the heart increased linearly with increasing jaw width. To reduce the average dose to the heart, the jaw width should be reduced as much as possible. Nilsson analysis of coronary angiography data from patients revealed that the location of coronary stenosis was correlated with the dose hotspot area³⁴. Therefore, along with the average dose, V40 and the maximum dose Dmax should be considered during actual treatment. However, as jaw width gradually decreased, the V40 volume and Dmax of the heart significantly increased; the mean dose to the heart in Plan0 was the lowest without increasing V40 or Dmax.

The dose to the contralateral breast is a key factor in the induction of second primary tumors during radiotherapy^{35,36}. The results of this study showed that with decreasing radiation jaw width, all the statistical indicators of the contralateral right breast increased to different degrees, but the index values of each plan group were generally lower. Therefore, the probability of a second primary tumor being induced by radiotherapy is lower.

Wang et al.³⁷ noted that the size of the lung V5 was an important predictor of radiation pneumonitis, and low-dose and high-volume lung radiation caused greater damage to lung function than did high-dose and low-

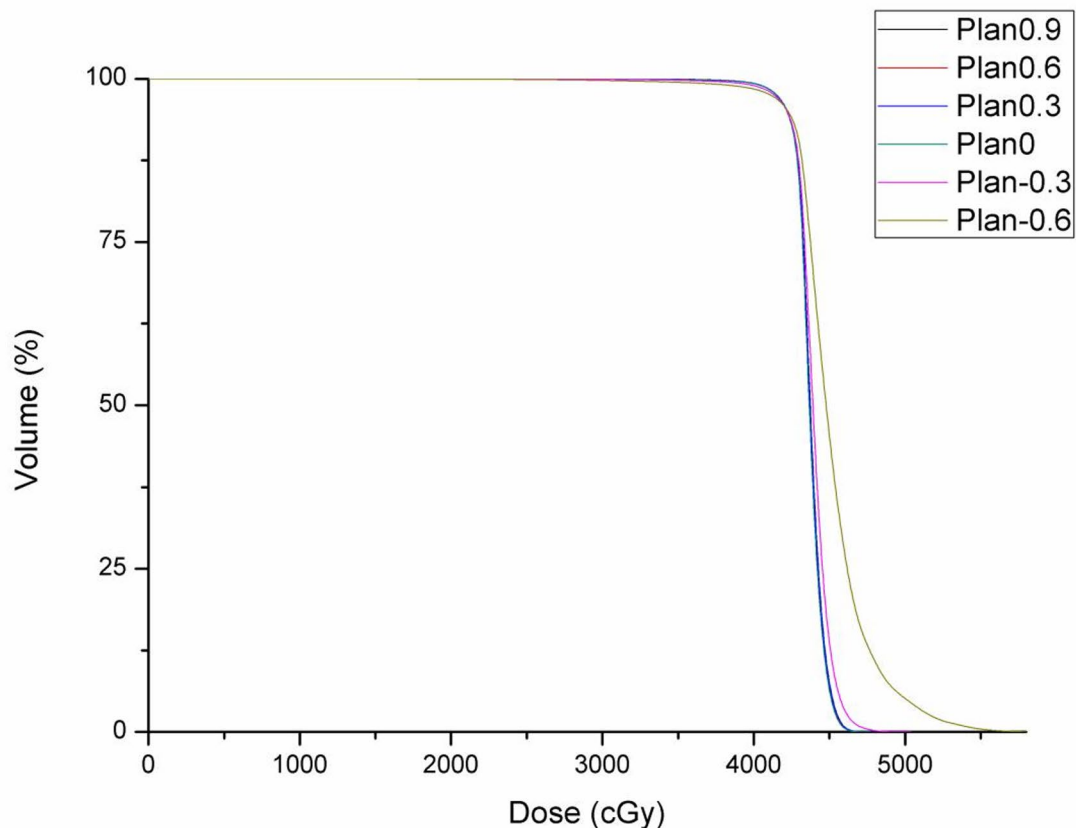


Fig. 4. The mean DVH for the PTV under the six plans.

volume lung radiation. Recht A et al. studied radiation-related lung injury caused by radiotherapy for breast cancer and reported that the risk of radiation pneumonitis caused by a relatively low dose of lung exposure to Volumes V5 and V10 after radiation was more important³⁸. Rodrigues et al. also proposed that the V20, V30, and Dmean of the ipsilateral lung are important parameters for predicting radiation pneumonitis after radiotherapy for breast cancer³⁹. This study revealed that the V5, V10, V20, and Dmean of the left lung were positively correlated with jaw width. Only for V30 was the difference between the six groups not statistically significant. Under the premise of ensuring dose coverage of the target volume, Plan0 can minimize the low-dose irradiation volume of the left lung.

The greatest limitation of the present study is that the sample size was relatively small. The optimal jaw width may be related to the total volume of the PTV, the curvature of the patient's thorax, the distance between the PTV and the heart, and the percentage of the lung in the tangential direction. The breathing pattern of the patient during treatment may also have an impact on the optimal jaw width. Compared with free breathing, deep inspiration and breath-holding can increase the lung volume while keeping the PTV away from the heart; ultimately, the optimal jaw width may be further reduced to better protect the surrounding normal tissues.

Although the individualized factors of the breast of the patient and the breathing pattern of the patient during the CT scan may have an impact on the optimal jaw width, the present study showed that relatively ideal dosimetry results could be obtained for the jaw widths corresponding to Plan0. In the initial optimization of radiotherapy plan for patients receiving left breast-conserving surgery, we can significantly reduce the number of repeated adjustments of the jaw width parameters by directly defining the internal boundary of the jaw at the half-beam field, thus greatly improving the efficiency of the radiotherapy plan and reducing the workload of radiotherapy medical dosimetrists.

In future studies, we will use this study and the method reported by Huang Y et al. as a basis from which to automate the search for VMAT jaw settings for each patient individually through the API scripting program and RapidPlan knowledge-based planning for large-sample data⁴⁰.

Conclusions

The internal boundary of the jaw set as 0 cm (Plan0) represents the optimal jaw width for the initial optimization of the plan design. This method is the simplest and most effective for radiotherapy planning for breast-conserving surgery for breast cancer as well as allows ideal dose distribution.

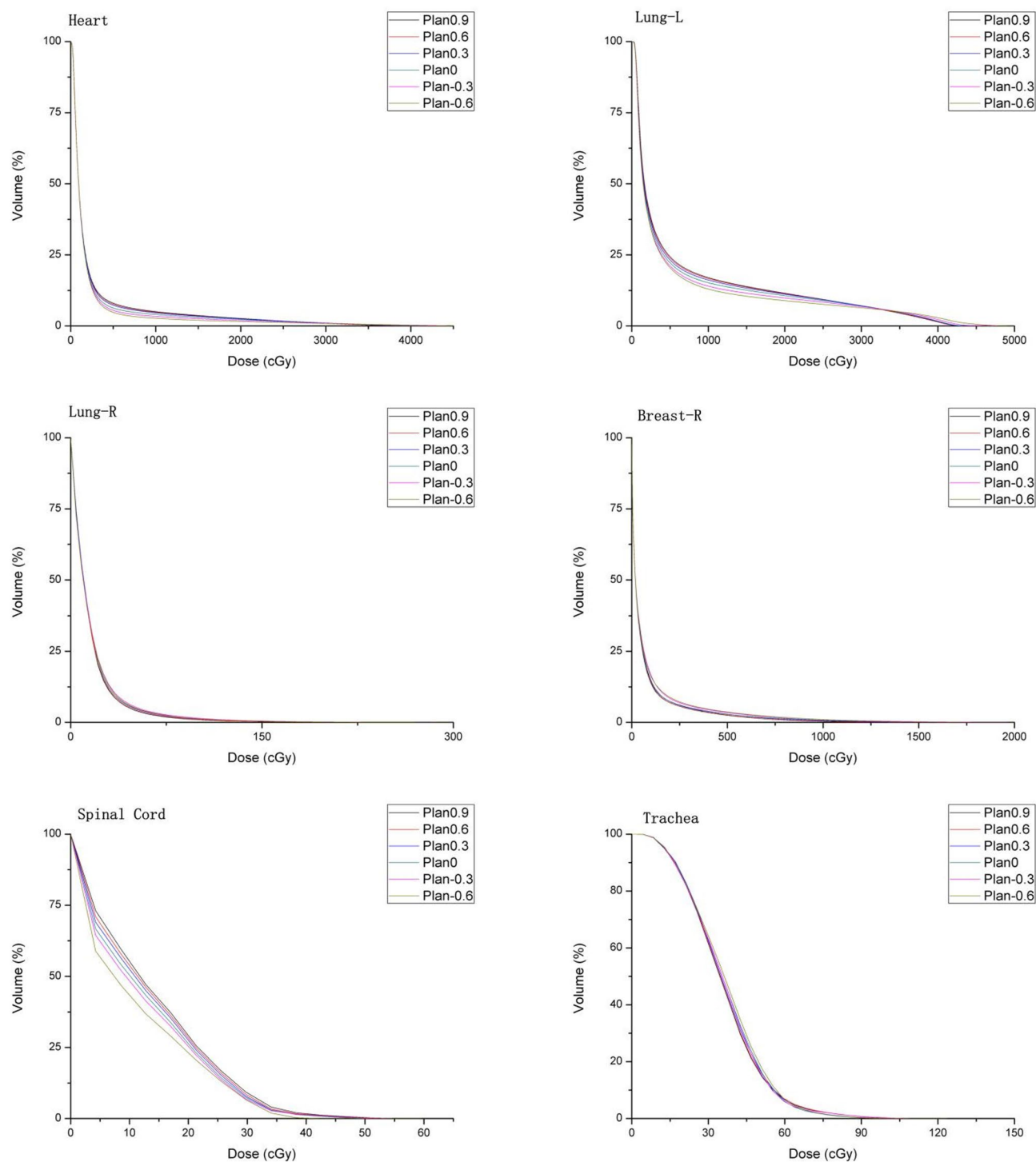


Fig. 5. The mean DVH for the heart, Lung-L, Lung-R, Breast-R, spinal cord, and trachea under the six plans.

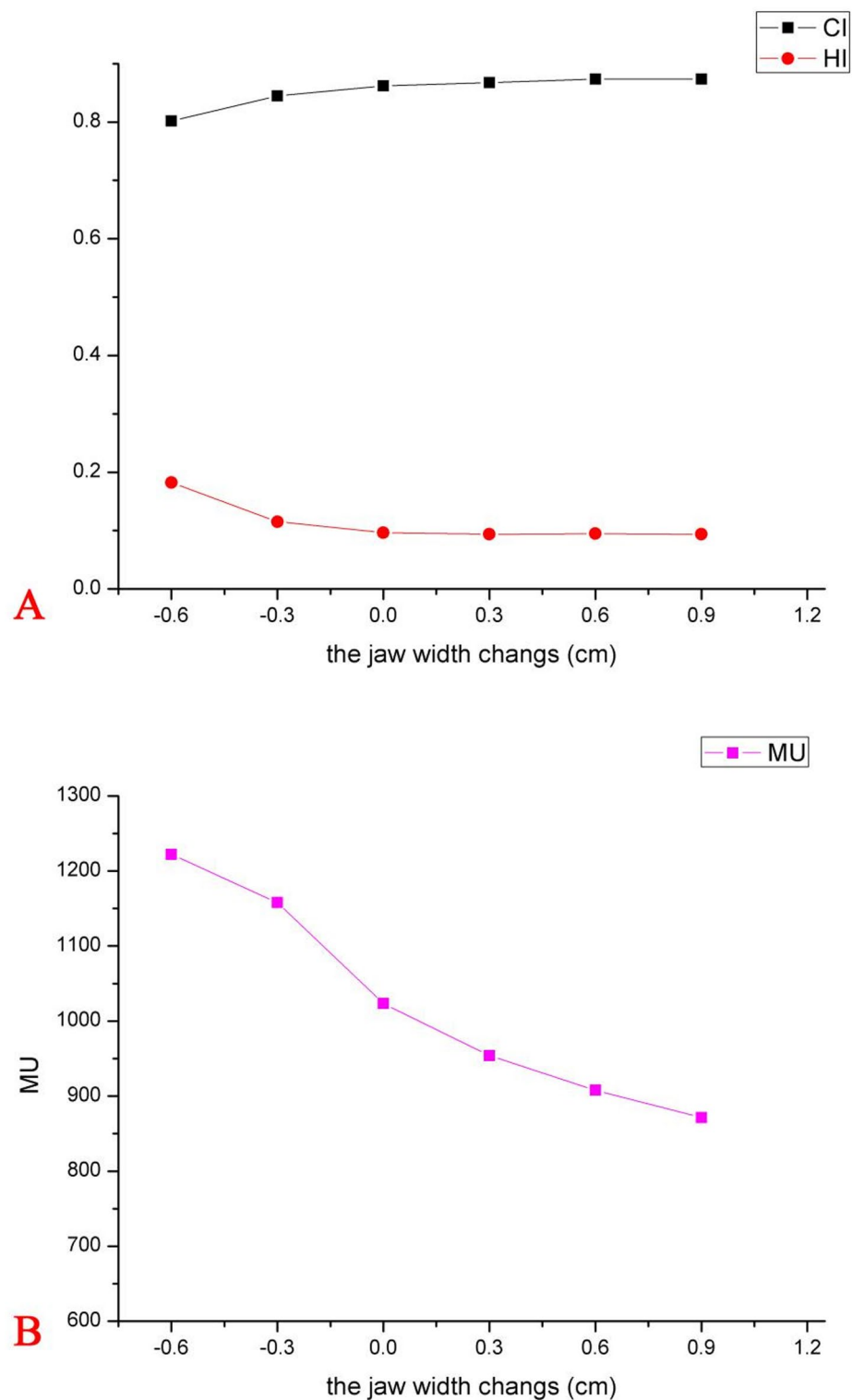


Fig. 6. The variation in the mean CI, HI, and MU versus jaw width. (A) The variation in the mean CI and HI versus jaw width. (B) The variation in the mean MU versus jaw width.

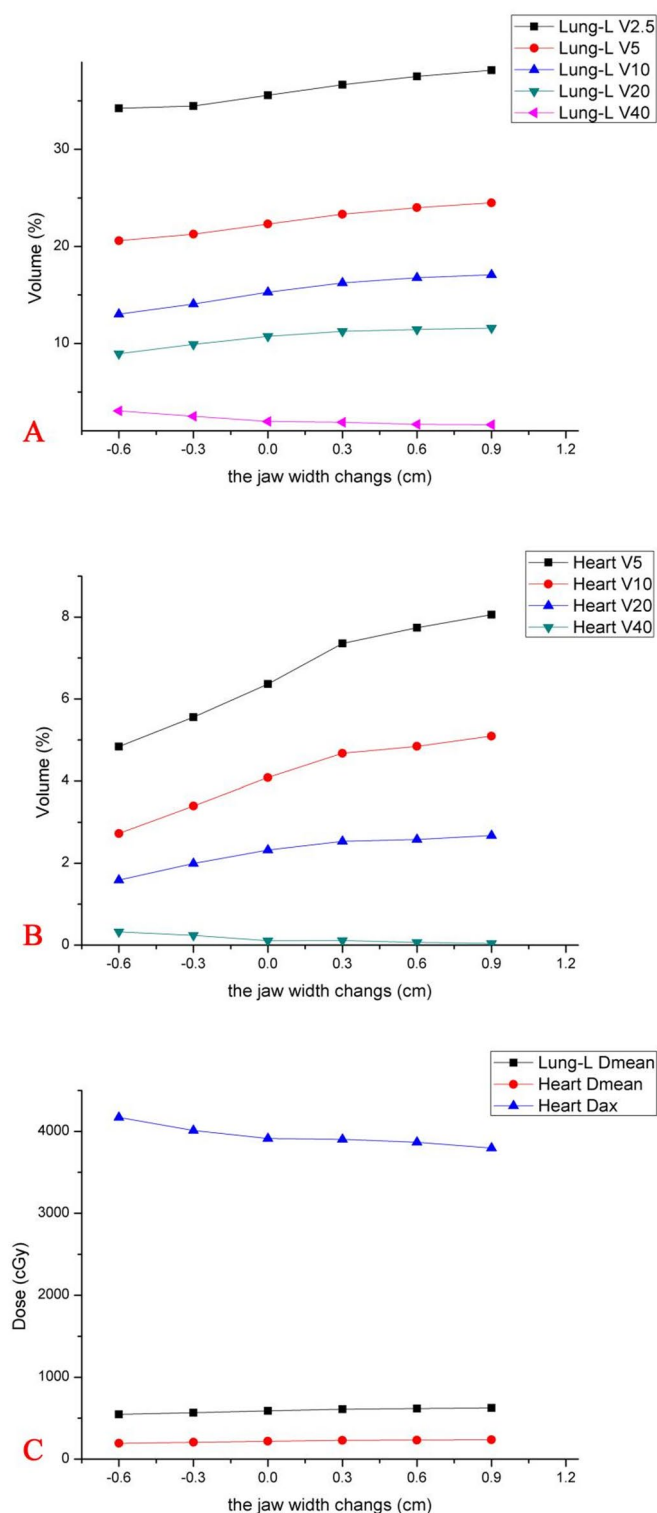


Fig. 7. Variations in each indicator of OARs on the ipsilateral side versus jaw width. (A) Variations in the mean volume of the left lung at doses of 2.5, 5, 10, 20, and 40 Gy versus jaw width. (B) Heart exposure mean volume at doses of 5, 10, 20, and 40 Gy versus jaw width. (C) Mean and maximum doses to the heart and left lung versus jaw width.)

Data availability

All data generated and analyzed during this study are included in this published article. The data that support the findings of this study are available from the corresponding author, Huai-wen Zhang, upon reasonable request.

Received: 6 March 2025; Accepted: 5 May 2025

Published online: 09 May 2025

References

1. Medical Policy and Administration Agency, National Health Commission of the People's Republic of China. Breast cancer treatment guidelines (2022 edition). *Chin. J. Oncol.* **45** (10), 803–833 (2023).
2. Wimmer, T. et al. Adherence to guidelines and benefit of adjuvant radiotherapy in patients with invasive breast cancer: results from a large population based cohort study of a cancer registry. *Arch. Gynecol. Obstet.* **299** (4), 1131–1140 (2019).
3. Darby, S. C. et al. Risk of ischemic heart disease in women after radiotherapy for breast cancer. *N. Engl. J. Med.* **368** (11), 987–998 (2013).
4. Furuya, T. et al. The dosimetric impact of respiratory breast movement and daily setup error on tangential whole breast irradiation using conventional wedge, field-in-field and irregular surface compensator techniques. *J. Radiat. Res.* **54** (1), 157–165 (2013).
5. Michalski, A. et al. A dosimetric comparison of 3D-CRT, IMRT, and static tomotherapy with an SIB for large and small breast volumes. *Med. Dosim.* **39** (2), 163–168 (2014).
6. Ma, J. et al. Post mastectomy Linac IMRT irradiation of chest wall and regional nodes: dosimetry data and acute toxicities. *Radiat. Oncol.* **8** (1), 81 (2013).
7. Bi, S., Zhu, R. & Dai, Z. Dosimetric and Radiobiological comparison of simultaneous integrated boost radiotherapy for early stage right side breast cancer between three techniques: IMRT, hybrid IMRT and hybrid VMAT. *Radiat. Oncol.* **17** (1), 60 (2022).
8. George, R. et al. Quantifying the effect of intrafraction motion during breast IMRT planning and dose delivery. *Med. Phys.* **30**, 552–562 (2003).
9. Hongo, H., Tokue, K., Sakae, T., Mase, M. & Omura, M. Robust Treatment Planning in Intrafraction Motion Using TomoDirect Intensity-modulated Radiotherapy for Breast Cancer. *In Vivo.* **35** (5), 2655–2659. (2021).
10. Zhang, Y. et al. A dosimetric and Radiobiological evaluation of VMAT following mastectomy for patients with left-sided breast cancer. *Radiat. Oncol.* **16** (1), 171 (2021).
11. Zhang, J. et al. Automatic VMAT on the left side Intensity-modulated radiotherapy planning. *Chin. J. Cancer Prev. Treat.* **28** (10), 753–758 (2021).
12. Feng, X. et al. Dosimetry study of three radiotherapy methods in whole milk, upper and lower clavicle and inner milk lymph node region after left breast conserving surgery. *Chin. J. Clin. Oncol.* **47** (8), 397–401 (2020).
13. Xu, B., Cao, Y. & Li, J. Dosimetry comparison between H-IMRT technique and H-VMAT technique in post-operative radiotherapy for breast adenocarcinoma. *J. Pract. Oncol.* **35** (6), 511–516. (2021).
14. Gao, Y. et al. Meta-analysis of the dose ratio between intensity modulated Arc therapy and intensity modulated radiotherapy after modified radical surgery for breast cancer. *Chin. J. Radiat. Oncol.* **30** (11), 1159–1166. (2021).
15. Virén, T. et al. Tangential volumetric modulated Arc therapy technique for left-sided breast cancer radiotherapy. *Radiat. Oncol.* **10**, 79 (2015).
16. Fogliata, A. et al. Critical appraisal of the risk of secondary Cancer induction from breast radiation therapy with volumetric modulated Arc therapy relative to 3D conformal therapy. *Int. J. Radiat. Oncol. Biol. Phys.* **100** (3), 785–793 (2018).
17. Thongsawad, S., Khamfongkhrua, C. & Tannanont, C. Dosimetric effect of jaw tracking in Volumetric-Modulated Arc therapy. *J. Med. Phys.* **43** (1), 52–57 (2018).
18. Sun, W. et al. Selection strategy of jaw tracking in VMAT planning for lung SBRT. *Front. Oncol.* **12**, 820632 (2022).
19. Jia, X., Dong, X. & Yue, K. Research on dosimetry and planning complexity of different jaw threshold in VMAT of na-sopharyngeal carcinoma based on jaw tracking technology. *China Med. Devices.* **37** (11), 34–38 (2022).
20. Wu, F. et al. Dosimetric study of 5 fixed-jaw techniques in volumetric modulated Arc therapy for nasopharyngeal carcinoma. *Chin. J. Med. Phys.* **37** (2), 133–137 (2020).
21. Liu, Y. et al. Effect analysis of different jaws widths in volume intensity modulated radiotherapy for cervical cancer. *J. Amry Med. Univ.* **45** (11), 1237–1242 (2023).
22. Boman, E. et al. A new split Arc VMAT technique for lymph node positive breast cancer. *Phys. Med.* **S1120-1797** (16), 30954–30951 (2016).
23. Rossi, M., Boman, E. & Kapanen, M. Contralateral tissue sparing in lymph node-positive breast cancer radiotherapy with VMAT technique. *Med. Dosim.* **44** (2), 117–121 (2019).
24. Su, J. et al. Design VMAT plan of left breast cancer postoperative radiotherapy based on TrueBeam platform. *Chin. J. Cancer Prev. Treat.* **29** (24), 1746–1752 (2022).
25. Kuo, L. C. et al. A VMAT planning technique for locally advanced breast cancer patients with expander or implant reconstructions requiring comprehensive postmastectomy radiation therapy. *Med. Dosim.* **44** (2), 150–154 (2019).
26. Chen, G. P. et al. A planning comparison of 7 irradiation options allowed in RTOG 1005 for early-stage breast cancer. *Med. Dosim.* **40** (1), 21–25 (2015).
27. Jin, K., Luo, J., Yu, X. & Guo, X. Hypofractionated radiotherapy with simultaneous tumor bed boost (Hi-RISE) in breast cancer patients receiving upfront breast-conserving surgery: study protocol for a phase III randomized controlled trial. *Radiat. Oncol.* **19** (1), 62 (2024).
28. National Cancer Center / National Cancer Quality Control Center Guideline of target delineation and treatment planning of adjuvant radiotherapy for breast cancer. *Chin. J. Radiat. Oncol.* **31** (10), 863–878 (2022).
29. Wang, S. L. F. H. et al. Hypofractionated versus conventional fractionated radiotherapy after breast-conserving surgery in the modern treatment era: a multicenter, randomized controlled trial from. *China J. Clin. Oncol.* **38** (31), 3604–3614 (2020).
30. Rossi, M., Virén, T., Heikkilä, J., Seppälä, J. & Boman, E. The robustness of VMAT radiotherapy for breast cancer with tissue deformations. *Med. Dosim.* **46** (1), 86–93 (2021).
31. Hodapp, N. The ICRU report 83: prescribing, recording and reporting photon-beam intensity-modulated radiation therapy (IMRT). *Strahlenther. Onkol.* **188** (1), 97–99 (2012).
32. Pasler, M. et al. VMAT techniques for lymph node-positive left sided breast cancer. *Z. Med. Phys.* **25** (2), 104–111 (2015).
33. Qiu, J. et al. Cardiac dose control and optimization strategy for left breast Cancer radiotherapy with Non-Uniform VMAT technology. *Technol. Cancer Res. Treat.* **20**, 15330338211053752 (2021).
34. Nilsson, G. et al. Distribution of coronary artery stenosis after radiation for breast cancer[J]. *J. Clin. Oncol.* **30** (4), 380–386 (2012).
35. Grantzau, T., Møllekjær, L. & Overgaard, J. Second primary cancers after adjuvant radiotherapy in early breast cancer patients: a National population based study under the Danish Breast Cancer cooperative group (DBCG). *Radiother. Oncol.* **106** (1), 42–49 (2013).
36. Yadav, B. S. et al. Second primary in the contralateral breast after treatment of breast cancer. *Radiother. Oncol.* **86** (2), 171–176 (2008).
37. Wang, S. et al. Analysis of clinical and dosimetric factors associated with treatment-related pneumonitis (TRP) in patients with non-small-cell lung cancer (NSCLC) treated with concurrent chemotherapy and three-dimensional conformal radiotherapy (3D-CRT). *Int. J. Radiat. Oncol. Biol. Phys.* **66** (5), 1399–1407 (2006).
38. Recht, A. et al. Lung dose-volume parameters and the risk of pneumonitis for patients treated with accelerated partial-breast irradiation using three-dimensional conformal radiotherapy. *J. Clin. Oncol.* **27** (24), 3887–3893 (2009).

39. Rodrigues, G. et al. Prediction of radiation pneumonitis by dose - volume histogram parameters in lung cancer—a systematic review. *Radiother. Oncol.* **71** (2), 127–138 (2004).
40. Huang, Y. et al. Fully automated searching for the optimal VMAT jaw settings based on eclipse scripting application programming interface (ESAPI) and rapidplan knowledge-based planning. *J. Appl. Clin. Med. Phys.* **19** (3), 177–182 (2018).

Author contributions

Huai-wen Zhang, Jing-hua Zhong and Hai-liang Guo conceived of the presented idea. Hai-liang Guo collected the data of all patients in this study. Huai-wen Zhang, Hao-wen Pang and Hai-liang Guo took the lead in writing the manuscript. All authors provided critical feed-back and helped shape the research, analysis, and manuscript.

Funding

We acknowledge funding from The Open Fund for Scientific Research of Jiangxi Cancer Hospital (number:2021J15).

Declarations

Competing interests

The authors declare no competing interests.

Ethics approval and consent to participate

This retrospective study was approved by the institutional review board of the First Affiliated Hospital of Gannan Medical University (No.LLSC2024067). Written informed consents were obtained from all patients prior to treatment.

Additional information

Correspondence and requests for materials should be addressed to J.-h.Z., H.-w.P. or H.-w.Z.

Reprints and permissions information is available at www.nature.com/reprints.

Publisher's note Springer Nature remains neutral with regard to jurisdictional claims in published maps and institutional affiliations.

Open Access This article is licensed under a Creative Commons Attribution-NonCommercial-NoDerivatives 4.0 International License, which permits any non-commercial use, sharing, distribution and reproduction in any medium or format, as long as you give appropriate credit to the original author(s) and the source, provide a link to the Creative Commons licence, and indicate if you modified the licensed material. You do not have permission under this licence to share adapted material derived from this article or parts of it. The images or other third party material in this article are included in the article's Creative Commons licence, unless indicated otherwise in a credit line to the material. If material is not included in the article's Creative Commons licence and your intended use is not permitted by statutory regulation or exceeds the permitted use, you will need to obtain permission directly from the copyright holder. To view a copy of this licence, visit <http://creativecommons.org/licenses/by-nc-nd/4.0/>.

© The Author(s) 2025